Human Molecular Genetics, 2008, Vol. 17, No. 15 **2310–2319**
doi:10.1093/hmg/ddn131
Advance Access published on April 18, 2008

Molecular dissection of ALS-associated toxicity of SOD1 in transgenic mice using an exon-fusion approach

Deng Han-Xiang[1,*], Jiang Hujun[1,5], Fu Ronggen[1], Zhai Hong[1], Shi Yong[1], Liu Erdong[1], Hirano Makito[1], C. Dal Canto Mauro[2] and Siddique Teepu[1,3,4]

[1]Davee Department of Neurology and Clinical Neurosciences, [2]Department of Pathology, [3]Department of Cell and Molecular Biology, [4]Institute for Neuroscience, Northwestern University Feinberg School of Medicine, Chicago, IL 60611, USA and [5]National Laboratory of Medical Genetics, Central South University, Changsha, Hunan, China

Received January 24, 2008; Revised and Accepted April 15, 2008

Mutations in Cu,Zn superoxide dismutase (SOD1) are associated with amyotrophic lateral sclerosis (ALS). Among more than 100 ALS-associated SOD1 mutations, premature termination codon (PTC) mutations exclusively occur in exon 5, the last exon of SOD1. The molecular basis of ALS-associated toxicity of the mutant SOD1 is not fully understood. Here, we show that nonsense-mediated mRNA decay (NMD) underlies clearance of mutant mRNA with a PTC in the non-terminal exons. To further define the crucial ALS-associated SOD1 fragments, we designed and tested an exon-fusion approach using an artificial transgene SOD1^{T116X} that harbors a PTC in exon 4. We found that the SOD1^{T116X} transgene with a fused exon could escape NMD in cellular models. We generated a transgenic mouse model that overexpresses SOD1^{T116X}. This mouse model developed ALS-like phenotype and pathology. Thus, our data have demonstrated that a 'mini-SOD1' of only 115 amino acids is sufficient to cause ALS. This is the smallest ALS-causing SOD1 molecule currently defined. This proof of principle result suggests that the exon-fusion approach may have potential not only to further define a shorter ALS-associated SOD1 fragment, thus providing a molecular target for designing rational therapy, but also to dissect toxicities of other proteins encoded by genes of multiple exons through a 'gain of function' mechanism.

INTRODUCTION

Mutations in the Cu, Zn-superoxide dismutase gene (*SOD1*) are associated with 20% of familial amyotrophic lateral sclerosis (ALS) cases (1,2). Transgenic mice overexpressing ALS-associated SOD1 mutants develop ALS-like disease, but transgenic mice overexpressing human wild-type SOD1 (hwtSOD1) or SOD1-deficient mice remain free of ALS-like phenotype, suggesting that mutant SOD1 causes the disease through the gain of a toxic property (3,4). We recently demonstrated that the conversion of mutant SOD1 from a soluble form to insoluble aggregates by crosslinking through intermolecular disulfide bonds via oxidation of cysteine residues in SOD1 is associated with ALS-like phenotype in transgenic mouse models, leading to a hypothesis that oxidation-mediated SOD1 aggregates underlie such a toxic property of mutant SOD1 (5,6). Further support for this hypothesis came from the observations that wild-type SOD1 could also be recruited into the insoluble aggregates by intermolecular crosslinking and this recruitment correlated with exacerbation of the disease or conversion to a disease phenotype (5,6). Two out of four cysteine residues in SOD1 are preferentially

*To whom correspondence should be addressed at: Davee Department of Neurology and Clinical Neurosciences, Northwestern University Feinberg School of Medicine, Tarry Building 13-715, 303 E. Chicago Ave, Chicago, IL 60611, USA. Tel: +1 3125034737; Fax: +1 3129080865; Email: h-deng@northwestern.edu

involved in this crosslinking process; one of such cysteines is Cys-146 (5,6). The preferential involvement of individual cysteines in SOD1 during the aggregate formation suggests that the amino acid sequences flanking cysteines and the conformation of SOD1 protein play a crucial role in determination of the crosslinking reactivity between cysteines during SOD1 aggregation upon oxidation.

Human *SOD1* is relatively a small gene with five exons in approximately an 11 kb genomic DNA fragment. Thus far >100 mutations, widely distributed in the SOD1 polypeptide and involving >70 of its 153 codons, have been identified in ALS. Most of the mutations result in substitution of amino acids. Nine mutations leading to premature termination codons (PTCs) in the last exon (exon 5), resulting in deletions of the C-terminus of SOD1, have been reported in ALS patients (www.alsod.org). No PTC in any exon other than exon 5 has been identified in ALS patients to date. Transgenic mice overexpressing some of the PTC mutations in the last exon developed an ALS-like phenotype, suggesting that an N-terminus polypeptide of 125 amino acids has sufficient toxicity to cause the motor neuron degeneration in mouse models (7).

Some types of human genetic diseases, including some neurodegenerative diseases, are caused by genetic mutations through a 'gain of function' mechanism. Understanding of the pathogenic mechanisms of these diseases is currently a major challenge. Previous studies have demonstrated that a full length mutant protein may not be an essential requirement for the development of disease, but the disease-associated toxicities may only lie in a crucial fragment of the protein. It is well established that amyloid-beta peptides (Abeta), as short as 40 to 42 amino acid derived from amyloid precursor protein of 695 amino acid, are the main constituents of amyloid plaques which are thought to be causal for the memory loss and cognitive decline in Alzheimer's disease (8). Similarly, a prion protein fragment of 106 amino acid out of the full length of 254 amino acid sufficiently supports pathogenic PrP^{sc} formation in transgenic mice (9). In mutant SOD1-mediated ALS, it has been proven that a C-terminal-truncated SOD1 protein of 125 amino acid out of a full length of 153 amino acid is sufficient to cause an ALS-like phenotype in transgenic mice (7). To further define smaller pathogenic fragments or protein domains may not only add to the understanding of the pathogenic mechanisms, but also facilitate minimization of the therapeutic targets (10), thus facilitating the design of rational therapies (11,12).

In the present study, we attempted to further define the ALS-associated toxicity of SOD1 by overexpressing shorter SOD1 polypeptides in transgenic mouse models. We encountered a technical challenge due to nonsense-mediated mRNA decay (NMD) mechanism. Therefore, we designed and tested an exon-fusion approach using an artificial transgene with a PTC at codon 116 in exon 4 of the human *SOD1* gene ($hSOD1^{T116X}$). Our data suggested that this approach may have powerful potentials for molecular dissection of the disease-associated toxicities of SOD1 and other proteins encoded by genes with multiple exons, thus to facilitate understanding the molecular basis of pathogenic mechanisms and designing therapeutic strategies.

RESULTS

NMD underlying clearance of mutant mRNA with premature stop codons of SOD1

Nine PTC mutations in *SOD1* have been reported in ALS patients. All of these PTCs exclusively occur in exon 5, the last exon of *SOD1*. No PTC mutation in any exon other than exon 5 has currently been reported, raising a possibility that a full-length polypeptide encoded by the first four exons may be required for the ALS-associated toxicity. In transgenic mice overexpressing some of the ALS-associated PTC mutants, it has been demonstrated that an N-terminal SOD1 polypeptide of 125 amino acid has sufficient ALS-associated toxicity (5,13–15). To understand the pathogenic mechanism of ALS and to further define crucial ALS-associated fragments of SOD1, we constructed two artificial transgenes using the human *SOD1* gene as a template. The transgene $hSOD1^{E77X}$ has a PTC at codon 77 in exon 3; while the transgene $hSOD1^{K91X}$ has a PTC at codon 91 in exon 4. Multiple copies of these transgenes were detected in the transgenic mice (Fig. 1A). However, *SOD1* mRNA was barely detected (Fig. 1B), and these transgenic mice remained free of ALS-like phenotype in their life time. The obviously lower mRNA expression in multiple lines of these transgenic mice, when compared to our previous *SOD1* transgenic mice harboring non-PTC mutations, suggests that mRNA transcribed from $hSOD1^{E77X}$ and $hSOD1^{K91X}$ transgenes was degraded (Fig. 1B). To test if the mRNA degradation was due to NMD, we first analyzed the transgene $hSOD1^{E77X}$ in cell culture models. Both *hwtSOD1* and $hSOD1^{E77X}$ transgenes were co-transfected at the same molar ratio into NIH/3T3 cells that were derived from a mouse embryonic fibroblast cell line. Resulting mRNA was reverse-transcribed to cDNA. Human transgene-derived SOD1 cDNA, but not mouse endogenous *SOD1* cDNA, was PCR-amplified using human-specific *SOD1* primers. The PCR product was sequenced. Dosage analysis was carried out based on the ratios of the peak height [mutant (T)/wt (G)] (refer to Materials and Methods) (Fig.1C and D). We found that the steady-state level of the mRNA transcribed from the $hSOD1^{E77X}$ transgene was $21.3 \pm 2.5\%$ of the hwtSOD1 transgene (Fig. 1E), suggesting that ~80% of $hSOD1^{E77X}$ mRNA was eliminated, if assuming that both transgenes were equally transfected, reverse transcribed and their mRNA was equally PCR-amplified. These results support the notion that mRNA carrying $hSOD1^{E77X}$ is committed to NMD. It is currently known that the NMD pathway is translation-dependent and inhibition of translation of mRNA with PTC will inhibit its NMD (16,17). To unequivocally prove that $hSOD1^{E77X}$ mRNA is degraded by this NMD pathway, we examined the mRNA ratio of $hSOD1^{E77X}$ to *hwtSOD1* by treating the transfected cells with cycloheximide. After 6 h treatment with cycloheximide, we found that the mRNA level of the $hSOD1^{E77X}$ was increased to $63.0 \pm 3.2\%$ of hwtSOD1 mRNA (Fig. 1E). These observations were corroborated using another cell line, NSC34, which is derived from mouse neural hybrid cells that exhibit some properties of motor neurons. We found that the mRNA level of the $hSOD1^{E77X}$ was $13.4 \pm 4.8\%$ of the hwtSOD1 mRNA in the group without cycloheximide treatment, and increased to

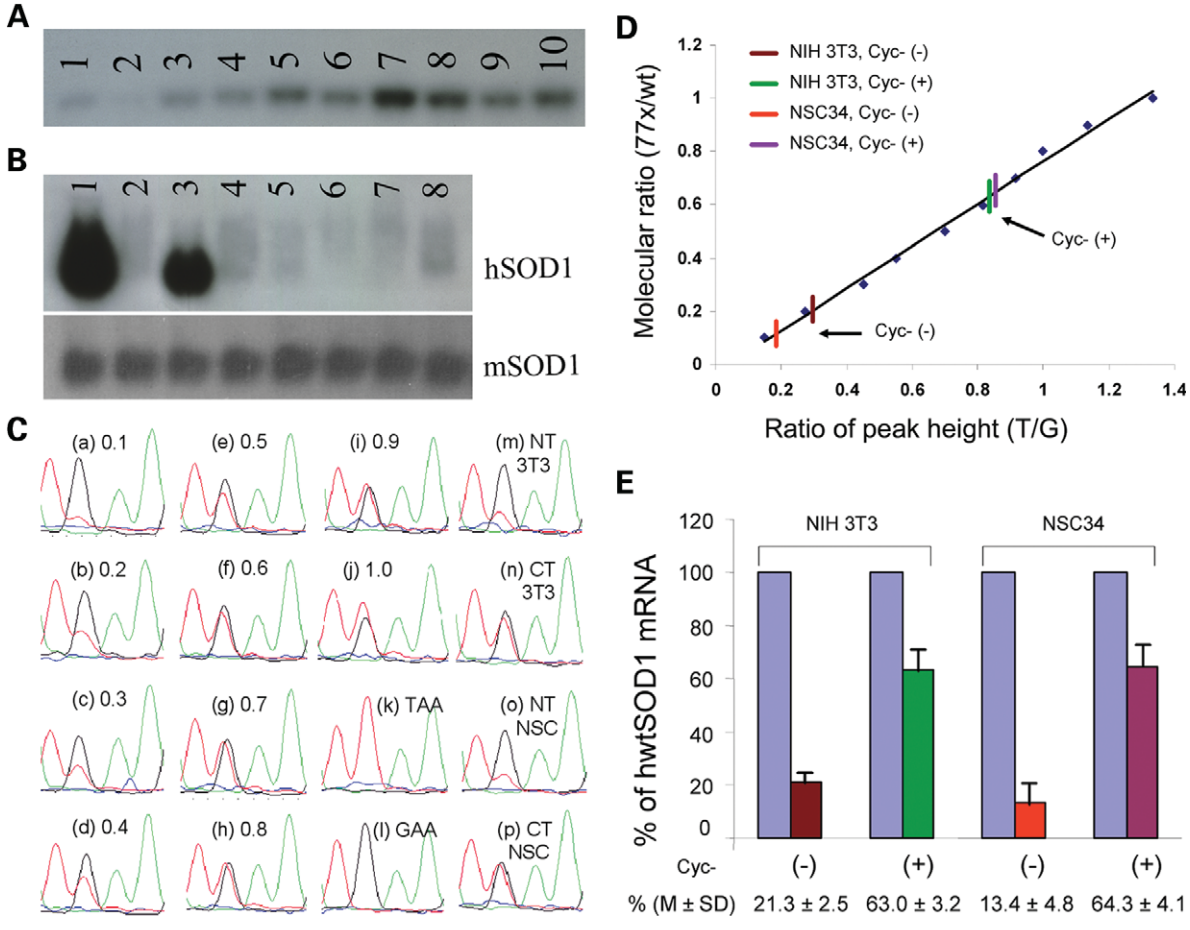

Figure 1. NMD underlying removal of mutant *SOD1* mRNA with PTCs in exons 3 and 4. (**A**) Southern blot showing that multiple copies of $hSOD1^{E77X}$ or $hSOD1^{K91X}$ transgene were integrated into mouse genome in the transgenic mice. Lane 2, human genomic DNA with two copies of SOD1 gene as a control; lanes 1 and 3–7, DNA from transgenic mice harboring transgene $hSOD1^{E77X}$; lanes 8–10, DNA from transgenic mice harboring transgene $hSOD1^{K91X}$. (**B**) The northern blot analysis of $SOD1^{E77X}$ and $SOD1^{K91X}$ transgenic mouse lines compared with established ALS mouse models of mutant SOD1. (Top panel) mRNA expression of human SOD1 transgenes detected by human SOD1-specific probe. (Low panel) mRNA expression of mouse endogenous SOD1 detected by mouse SOD1-specific probe as an internal control. Lane 1, $SOD1^{G93A}$ transgenic mice that develop disease around 100 days. Lane 2, wild-type mouse (non-transgenic) as a control. Lane 3, $SOD1^{L126Z}$ transgenic mice that develop disease around 350 days. Lanes 4–7, $SOD1^{E77X}$ transgenic mice. Lane 8, $SOD1^{K91X}$ transgenic mice. (**C**) Representative sequence electropherograms showing NMD of $SOD1^{E77X}$. Plasmid DNA containing cDNA of SOD1 with $SOD1^{E77X}$ mutation was mixed with plasmid containing wild-type cDNA of SOD1 at 10 different ratios by amount, i.e. from 0.1 to 1.0 (mutant/wild-type). Mixed DNA samples were used as templates for PCR-sequencing. The relative ratio of the peak height (T/G) was established by measuring the individual peak heights representing $SOD1^{E77X}$ (T) and wtSOD1 (G). The known molecular ratios (0.1–1.0) of the mutant/wild-type are labeled on the top of the sequence electropherograms of the sub-panels (A–j). Sub-panel (k) shows a sequence electropherogram of a stop codon (TAA) at codon 77, and (l) shows wtSOD1 at codon 77 when a single type of DNA was used. Sub-panels (m and n) show the sequence electropherograms of RT-PCR product of human SOD1 from NIH/3T3 cells transfected with equal molar ratio of $SOD1^{E77X}$/wtSOD1 plasmids; CT, cycloheximide-treated; NT, not treated with cycloheximide. Sub-panels (o) and (p) show the sequence electropherograms of RT–PCR product of human SOD1 from another cell line (NSC34) transfected with equal molar ratio of $SOD1^{E77X}$/wtSOD1 plasmids. (**D**) A standard curve showing ratios of peak height (T/G) against known molecular ratios ($SOD1^{E77X}$/wtSOD1). Cyc- (+), cycloheximide-treated; Cyc- (−), not treated with cycloheximide. (**E**) Relative steady-state mRNA levels of $SOD1^{E77X}$ in cell lines of NIH/3T3 and NSC34 compared with wtSOD1. Approximately 80% of mRNA transcribed from human $SOD1^{E77X}$ was eliminated, and inhibition of translation by cycloheximide significantly suppressed such elimination in both NIH/3T3 and NSC34 cell lines (Student's *t*-test, $P < 0.001$).

64.3 ± 4.1% of hwtSOD1 mRNA when treated with cycloheximide (Fig. 1E). We further verified these observations by sequencing analysis of SOD1 cDNA clones (Supplementary Material, Fig. S1).

In addition to $hSOD1^{E77X}$ that has a PTC in exon 3, we also analyzed the transgene $hSOD1^{K91X}$ that has a PTC in exon 4. We observed that ∼80% of $hSOD1^{K91X}$ mRNA was decayed and that inhibition of protein translation by cycloheximide significantly suppressed such decay in both NIH/3T3 and NSC34 cells (Supplementary Material, Fig. S2), suggesting that SOD1 mRNA containing a PTC in exon 4 is also committed to NMD. Thus, our data have provided multiple lines of evidence that $hSOD1^{E77X}$ and $hSOD1^{K91X}$ mRNAs are degraded by NMD. This mechanism may also underlie degradation of other mutant *SOD1* mRNAs containing a PTC in exons 1–4, the non-terminal exons of *SOD1*, as NMD appears to be a universal mechanism of the cellular defense against the potentially deleterious effects of truncated proteins (16). This notion may reflect the current observation that there is no PTC mutation identified in any exon other than

exon 5, although more than 100 mutations involving over 70 codons have been reported. Since NMD may degrade the *SOD1* mRNA with PTC in exons other than exon 5, leading to a significantly reduced protein amount, therefore, an insufficient amount of the mutant protein may not be able to cause the disease, even if a C-terminal truncated SOD1 polypeptide has ALS-associated toxicity.

mRNA with a PTC in the last fused exon escaping NMD

Since SOD1-mediated ALS in transgenic mice is dosage-dependent (3,18,19), and NMD affects ~80% of the *SOD1* mRNA with a PTC, thus preventing high expression of the mutant SOD1, it becomes a technical challenge for defining the ALS-associated polypeptide or domain further upstream in SOD1. To overcome this difficulty, we designed an exon-fusion approach. Based on the current understanding of NMD, if intron 4, the last intron of *SOD1* is deleted and the last two exons are fused together to become the last exon, then any mRNA with a PTC in exon 4 should be able to escape NMD. To test this strategy, we deleted the 1.1 kb intron 4, so that exons 4 and 5 were fused together as the last exon. Previous studies suggest that two out of four cysteines in SOD1 are predominantly involved in SOD1 aggregation *in vivo*; one of which is Cys146 (5). The other cysteine remains undefined. Since our initially tested transgenes E77X and K91X do not include Cys111, which may play an important role in ALS pathogenesis, we tested a transgene SOD1^{T116X} that includes all three untested cysteines (Cys6, Cys57 and Cys111). This PTC was located in the previous exon 4 and now in the last fused exon (*hSOD1*^{T116X}). We first tested this transgene in cell culture models, and found that the mRNA levels of *hSOD1*^{T116X} were about half of that of *hwtSOD1* in both cellular models (Fig. 2A and B). Since intron 4 may contain some transcription regulation elements, the reduction of *hSOD1*^{T116X} mRNA may not be due to NMD, but due to reduced transcription. To test this possibility, we analyzed the mRNA levels of *hSOD1*^{T116X} from the cycloheximide-treated groups. Our data demonstrated that inhibition of protein translation did not significantly alter the levels of *hSOD1*^{T116X} mRNA (Fig. 2A and B). These observations were further corroborated by sequencing analysis of the recombinant clones (Supplementary Material, Fig. S1). The cycloheximide treatment did not significantly increase the steady-state levels of hSOD1^{T116X} mRNA, supporting the idea that the reduction of *hSOD1*^{T116X} mRNA is not due to NMD but most likely due to reduced transcription and/or other mechanisms.

Development of ALS-like phenotype in transgenic mice overexpressing HSOD1^{T116X}

Since the *hSOD1*^{T116X} transgene yielded approximately half of the steady-state mRNA level compared with the *hwtSOD1* transgene, transgenic mice overexpressing hSOD1^{T116X} may develop ALS phenotype if truncated protein hSOD1^{T116X} still has ALS-associated toxicity, and if its expression is high enough. To test this possibility, we developed transgenic mice overexpressing hSOD1^{T116X}. The *hSOD1*^{T116X} transgenic mice had relatively lower mRNA expression from the

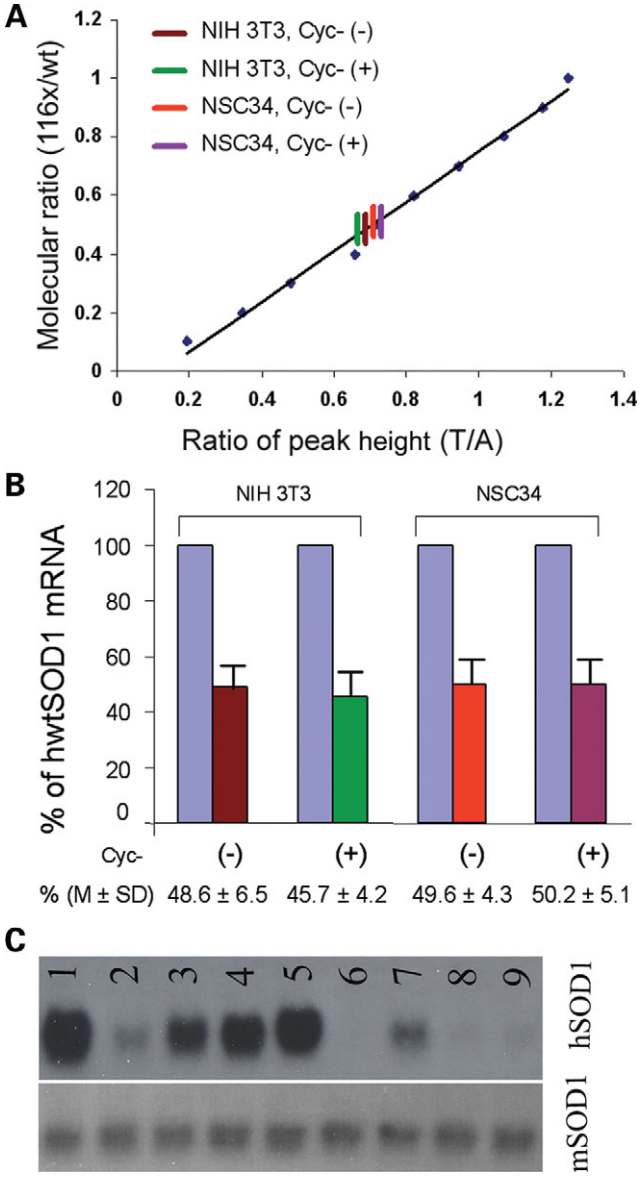

Figure 2. Escape of NMD via exon-fusion approach. (**A**) A standard curve showing ratios of peak height (T/A) against known molecular ratios (hSOD1^{T116X}/hwtSOD1). (**B**) Relative steady-state mRNA levels of hSOD1^{T116X} in cell lines of NIH/3T3 and NSC34 represent approximately half of hwtSOD1 mRNA. However, inhibition of translation by cycloheximide does not affect the steady-state mRNA level of hSOD1^{T116X} in either NIH/3T3 or NSC34 cell line (Student's *t*-test, $P > 0.5$). (**C**) The northern blot analysis of *hSOD1*^{T116X} transgenic mouse lines compared to established ALS mouse models of mutant SOD1. Lane 1, *SOD1*^{G93A} mice that develop disease by 100 days. Lane 2, *SOD1*^{A4V} low expressor line that never develops disease, even when crossed with *hwtSOD1* transgenic mice. Lane 3, *SOD1*^{A4V} high expressor line that do not develop disease alone. However, they will develop disease by 8 months when crossed with the *hwtSOD1* transgenic mice (6). Lane 4, *hwtSOD1* transgenic mice that do not develop disease (3). Lane 5, *SOD1*^{L126Z} high expressor line that develops disease by 12 months. They will develop disease by 6 months when crossed with *hwtSOD1* transgenic mice (5). Lane 6, *SOD1*^{L126Z} low expressor line that never develops disease even when crossed with *hwtSOD1* transgenic mice. Lane 7, *SOD1*^{T116X} high expressor line that develops disease by 10 months in the homozygous state (double dose). They will develop disease by 13–18 months when crossed with *hwtSOD1* transgenic mice. Lanes 8 and 9, *SOD1*^{T116X} low expressor lines that do not develop disease in their life time.

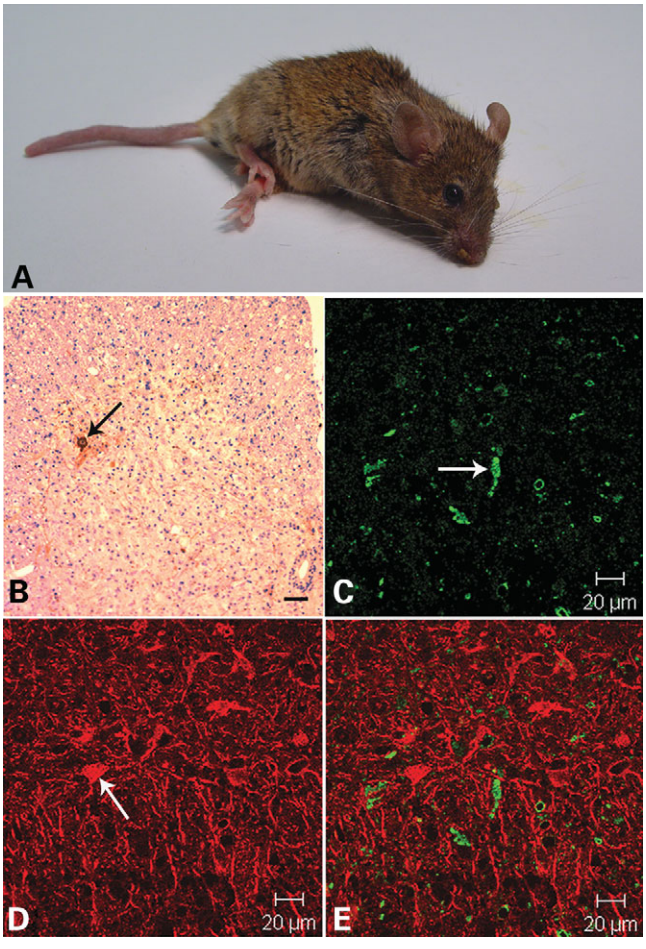

Figure 3. Development of ALS-like phenotype and pathology in the *hSOD1*^{T116X} transgenic mice. (**A**) *hSOD1*^{T116X}*/hwtSOD1* double transgenic mice showing ALS-like phenotype, including motor impairment, paralysis, muscle atrophy (especially in the hind legs) and loss ~30% of body weight by the end-stage. (**B**) A representative section showing severe loss of motor neurons in the anterior horn of lumbar spinal cord. Immunohistochemistry using an antibody against ChAT shows a ChAT-positive motor neuron (arrow). An average number of motor neurons in the L1 to L3 segments in an affected mouse that we analyzed in detail was 6.4 ± 2.6 per anterior horn, compared to 14.6 ± 4.3 per anterior horn in a control (Student's *t*-test, $P < 0.001$); bar, 100 μm. (**C**–**E**) Confocal microscopy showing SOD1 aggregates (green in C) and astrocytosis (D) in spinal cord sections of affected mice. Astrocytes are shown as glial fibrillary acidic protein-positive cells in red (D). No apparent SOD1 aggregates have been observed in astrocytes (overlay in E).

hSOD1^{T116X} transgene when compared with our previously established ALS mouse models overexpressing other SOD1 mutants (Fig. 2C). The hemizygous mice did not develop an ALS-like phenotype in their life time. To increase the hSOD1^{T116X} expression, we interbred the *hSOD1*^{T116X} hemizygous mice. We obtained one possible *hSOD1*^{T116X} homozygous mouse out of six transgene-positive pups from a single interbreeding (Supplementary Material, Fig. S3). This mouse developed ALS-like phenotype that was very similar to disease phenotype observed in the other transgenic mice overexpressing SOD1^{G93A}, SOD1^{A4V} or SOD1^{L126Z}, resulting in premature death by 10 months with a disease duration of 2 weeks.

Since the integration of the transgene into the mouse genome may interrupt a gene function, loss of such a function in homozygotes may contribute to ALS-like phenotype. To exclude this possibility and to further verify that hSOD1^{T116X} is toxic, we generated *hSOD1*^{T116X}*/hwtSOD1* double transgenic mice. We have previously demonstrated that hwtSOD1 could convert the unaffected phenotype in *SOD1*^{A4V} mice to ALS-like phenotype in *SOD1*^{A4V}*/hwtSOD1* double transgenic mice in a mutant dose-dependant manner (5). This phenomenon is associated with the conversion of the hwtSOD1 to insoluble aggregates through intermolecular disulfide bonds (5,6). We obtained five double transgenic mice (*hSOD1*^{T116X}*/hwtSOD1*) and these mice developed ALS-like phenotype and died of the disease by 13–18 months, with disease duration of 2–3 weeks (Fig. 3A, and Supplementary Material, Fig. S4). Over half of the motor neurons in the anterior horns of lumbar segment were lost (Fig. 3B). Similar to ALS mouse models overexpressing other SOD1 mutants, immuno-reactive SOD1 aggregates and astrocytosis were apparent in these affected mice (Fig. 3C–E). Consistent with our previous observation (5), hwtSOD1 was shown to be recruited into SOD1 aggregates using an antibody (c-SOD1) against the C-terminal polypeptide (5) that is deleted in truncated hSOD1^{T116X} protein (Fig. 4). These aggregates were largely present in neuritic processes and some surviving large neurons (Fig. 4A and B). These aggregates also included ubiquitin (Fig.4C–E) and were prominent in anterior root axons (Fig. 4F–H).

DISCUSSION

The toxic properties of mutant SOD1 has been examined using various conditions *in vitro* and *in vivo* (7,20–26). Different approaches have various advantages and drawbacks. Compared with an *in vivo* approach, the *in vitro* approach is less time-consuming and many influential factors may be controlled. The *in vitro* approach has provided significant information for understanding the biophysical and biochemical properties of SOD1 mutants. However, because ALS is a clinical diagnosis of a complex disease process and many different cell types may be involved in the pathogenesis (19,27–33), the disease process may not be adequately modeled using *in vitro* systems. Thus, whether a specific property identified *in vitro* has significant pertinence to the pathogenesis of ALS remains to be further addressed. A challenging example is that all four cysteines in SOD1 have been found to be reactive in the intermolecular crosslinking by disulfide bonds, leading to SOD1 aggregation under oxidative conditions *in vitro* (6). However, it seems that only two of the four cysteines significantly contributed to SOD1 aggregation by this crosslinking in mouse models during the disease process (5,6). Alternatively, the use of chick embryo spinal cords has been shown to be a sensitive tool to analyze SOD1 aggregates and neural cell death (34), but it is yet to be determined if neural cells in an embryonic stage share the same properties as adult neurons. Furthermore, axonal degeneration rather than neuronal cell death *per se* may be the primary pathology that triggers the ALS symptoms (35,36). Using *SOD1* cDNA transgene under the control of other gene promoters is another alternative choice to characterize the SOD1 toxicity in a mouse model

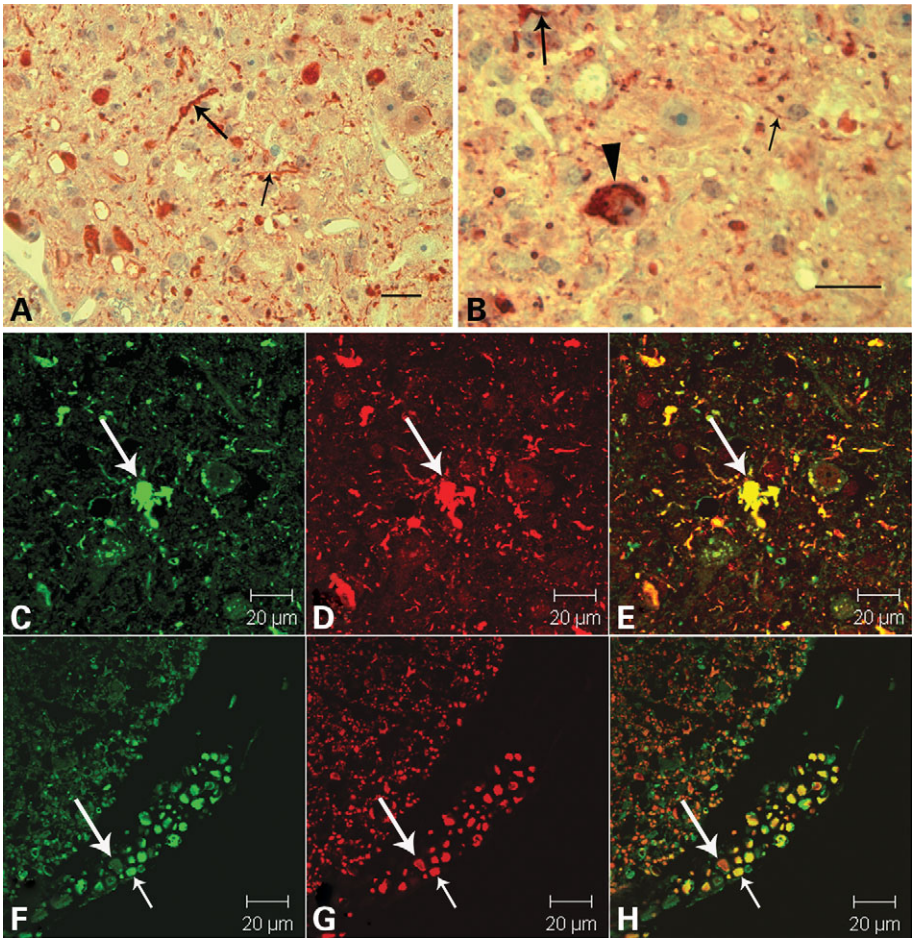

Figure 4. Recruitment of wtSOD1 into aggregates in spinal cord and anterior root axons of *hSOD1*^{T116X}*/hwtSOD1* double transgenic mice. (**A** and **B**) Immunohistochemical staining with an antibody against the last 28 amino acid of SOD1 (c-SOD1) (5) showed a large number of wtSOD1 aggregates in the spinal cord sections of the affected mice (A and B). These aggregates were predominantly present in neuritic processes (arrows). Some wtSOD1 aggregates were found in surviving large neurons (arrowhead in B). Some neuritic processes with wtSOD1 aggregates were apparently swollen (large arrows in A and B). (**C**–**E**) Immunoreactive SOD1 aggregates containing ubiquitin. Confocal microscopy showing c-SOD1-positive aggregates (green in C) and ubiquitin (red in D) in spinal cord sections of affected mice. Signals from SOD1 and ubiquitin largely overlapped (overlay in E). (**F**–**H**) Prominent SOD1 aggregates in anterior root axons. Confocal microscopy showing c-SOD1-positive aggregates (green in F) in anterior root axons with neurofilament medium chain staining (red in G) in the spinal cord sections of affected mice. Compared with axons in the neighboring spinal cord, the anterior root axons had more prominent SOD1 aggregates. A representative anterior root axon without apparent SOD1 aggregates is shown by a large arrow, and a representative anterior root axon with SOD1 aggregates is shown by a small arrow. Most of the anterior root axons showed prominent SOD1 aggregates (overlay in E).

(37), as this strategy should escape NMD. But it is unknown if the different gene expression profiles driven by other promoters have significant influence on the pathogenesis of the disease. The genomic SOD1 transgenes may have authentic expression profiles, but NMD prevents further characterization of the mutants with PTCs upstream of exon 5.

NMD is an RNA surveillance pathway that destroys aberrant mRNAs containing PTCs, so that cells can be protected from the deleterious effects of the truncated proteins (16). We used *SOD1* promoter to drive *SOD1* cDNA expression, so that NMD could be bypassed. However, this approach did not yield enough SOD1 expression (data not shown), suggesting that *SOD1* introns have important transcriptional regulatory elements required for high expression. Therefore, we deleted the last intron. Although deletion of the last intron resulted in reduction of approximately half of the *SOD1* mRNA in cell culture, we speculated that such a reduction in expression may still be sufficient to cause ALS-like phenotype in homozygous mice if the truncated SOD1 has ALS-associated toxicity. Development of the ALS-like phenotype and pathology in the *SOD1*^{T116X} homozygous and *SOD1*^{T116X}/hwtSOD1 mice demonstrates that an N-terminus polypeptide of only 115 amino acid has sufficient toxicity to cause ALS. This is the shortest ALS-associated SOD1 molecule currently defined in ALS mouse models (7). Although we did not narrow down the toxic fragment substantially, our data have provided proof-of-principle evidence that the exon-fusion approach has promising potential for further defining the toxic SOD1 fragment that is crucial for triggering ALS and thus as a molecular target for designing rational therapy. This approach may also have general applications to molecular dissection of the disease-associated toxicities of other proteins, which are encoded by genes with multiple exons, with a ‘gain of function’ mechanism.

Truncated SOD1 is extremely unstable in soluble fraction of the cells. Previous studies demonstrated that truncated $SOD1^{L126Z}$ was present as insoluble aggregates and was virtually undetectable in the soluble fraction in the affected ALS mice (5,14,15), suggesting that the insoluble SOD1 aggregates, rather than the soluble form of SOD1 are causally associated with the disease. We have previously shown that wtSOD1 can be recruited into SOD1 aggregates when ALS-associated mutant SOD1 is present; this recruitment can either exacerbate the disease in $SOD1^{G93A}$ and $SOD1^{L126Z}$ mice or convert the phenotype from unaffected to affected status in $SOD1^{A4V}$ mice (5). By crossbreeding the unaffected $SOD1^{T116X}$ hemizygous mice with *hwtSOD1* mice, we have showed in the present study that wtSOD1 can also convert $SOD1^{T116X}$ mice from an unaffected to affected status. This phenotypic transition is related to conversion of wtSOD1 into aggregates, as shown by antibody c-SOD1 in immunohistochemistry and confocal microscopy. Thus, our data suggest that recruitment of wtSOD1 into aggregates, thereby exacerbating the disease or converting to the disease status, may be a common phenomenon. This phenomenon, in turn, provides further support to the hypothesis that SOD1 aggregates are ALS-associated toxic species, regardless of whether they are composed of mutant or wild-type SOD1 (5).

The current consensus regarding the mechanism of how mutant SOD1 causes ALS is that mutant SOD1 becomes toxic through gain of either a normal function or a novel toxic property. The additive effect of wtSOD1 aggregates on the mouse phenotype supports a hypothesis that wtSOD1 *per se* also has an endogenous ALS-associated toxicity; this endogenous toxicity is enhanced by mutations; this endogenous toxicity is likely derived from the propensity to SOD1 aggregation. This hypothesis is supported by the observations that (i) overexpression of ALS-associated SOD1 mutants in transgenic mice over a certain level causes ALS-like phenotype, but overexpression of wtSOD1 at a comparable level does not lead to ALS-like phenotype (3,18); (ii) SOD1 aggregation seems a common pathological feature in ALS mouse models (5,7); (iii) recruitment of wtSOD1 into the aggregates exacerbates the disease in $SOD1^{G93A}$ and $SOD1^{L126Z}$ mice or converts the phenotype from unaffected to affected status in $SOD1^{A4V}$ (5) and the newly developed $SOD1^{T116X}$ mice; (iv) both wtSOD1 and ALS-associated SOD1 mutants have the propensity to aggregation *in vitro*, with wtSOD1 having a lower propensity to aggregation than the ALS-associated mutant SOD1 (6); (v) wtSOD1 can form heterodimers/heteromultimers with mutant SOD1, and homodimers and homomultimers alone through intermolecular disulfide bonds in the $SOD1^{L126Z}$/hwtSOD1 double transgenic mice with exacerbated disease (5,6).

During SOD1 aggregation in the disease process, two out of four cysteines are predominantly oxidized (5). The preferential involvement of cysteines in SOD1 suggests that the amino acid sequence flanking cysteines and the overall conformation of the polypeptide play an important role in the determination of the crosslinking reactivity of individual cysteines *in vivo*. Since a truncated SOD1 polypeptide with only one reactive cysteine is sufficient to form SOD1 dimers and cause the disease (5), a minimum N-terminal SOD1 polypeptide that is essential for ALS-associated toxicity may be further defined. Meanwhile, it is also possible that another SOD1 polypeptide of the C-terminus with a reactive Cys146 is able to form SOD1 dimers and cause ALS. Further investigation of these possibilities in mouse models may provide important clues for understanding the molecular mechanism of SOD1 aggregation *in vivo* and the pathogenesis of mutant SOD1-mediated ALS in humans. The observations that no PTC mutation has been identified in any exon other than exon 5 of SOD1 in ALS patients, and that $SOD1^{T116X}$ mice develop ALS-like phenotype and pathology may provide a vivid example that NMD is an important mechanism to protect cells from the deleterious effects of a truncated protein (16).

MATERIALS AND METHODS

Construction of human *SOD1* transgenes

Three transgenes ($hSOD1^{E77X}$, $hSOD1^{K91X}$ and $hSOD1^{T116X}$) were constructed. A 7 kb *Pvu*II/*Bam*HI fragment containing exons 2, 3 and 4 and mutant exon 5 in a pBluescript plasmid vector was used as a template for PCR to introduce PTCs (E77X or K91X) into exon 3 or 4 by site-directed mutagenesis (Stratagene, La Jolla, CA, USA). Primer hSOD1-K77Xf (5′-ggtgggccaaaggattaagagaggcatgttg-3′) was used to introduce a PTC in exon 3, and primer hSOD1-K91X (5′-caatgtgactgctgactaagatggtgtggccga-3′) in exon 4, respectively. The entire construct was assembled by ligation of a 4.6 kb *Eco*RI/*Pvu*II fragment containing exon 1 and the 7 kb *Pvu*II/*Bam*HI fragment containing the E77X or K91X mutation into the pBluescript plasmid vector. For construction of transgene $SOD1^{T116X}$, intron 4 was deleted with primer $hSOD1^{delI4}$ (5′-cattggccgcacactgcatgaaaaagcagat-3′) and a PTC was introduced into exon 4 at codon 116 with primer $hSOD1\text{-}T116X^{delI4}$ (5′-tgcatcattggccgctaacat gaaaaagcagat -3′). Deletion of the 1.1 kb intron 4 resulted in a fusion of exons 4 and 5. Then the 5.9 kb *Pvu*II/*Bam*HI fragment without intron 4 was ligated with the 4.6 kb *Eco*RI/*Pvu*II fragment containing exon 1 to assemble into transgene $hSOD1^{T116X}$. The plasmids containing these transgenes were propagated in *Escherichia coli* XL 1 blue. The DNA sequence of the transgenes was verified by sequencing.

Cell culture and transfections

NIH/3T3 and NSC 34 cells, both derived from mouse cell lines, were grown in Dulbecco's modified Eagle's medium in 6-well plates. Transient transfections were performed using SuperFect Transfection reagent (Qiagen, Valencia, CA, USA). Plasmid DNA containing the *hwtSOD1* gene was mixed with plasmid DNA containing a mutant *SOD1* gene ($hSOD1^{E77X}$, or $hSOD1^{K91X}$) in equal amounts (2 μg each). The hwtSOD1 plasmid was mixed with plasmid containing $hSOD1^{T116X}$ at a ratio of 1:0.924 (2 and 1.85 μg, respectively). This ratio was calculated based on the different molecular weight of the plasmids, so that the molar concentration of the hwtSOD1 and $hSOD1^{T116X}$ during transfections would remain the same. The transfected cells in the 6-well plates were divided into two groups. The cells in the lower three wells were treated with cycloheximide (200 μm) and the cells in the top three wells were not cycloheximide-treated.

In the cycloheximide-treated group, the transfected cells were cultured for 16 h and then cycloheximide was added. Cells were harvested 6 h later. In the non-cycloheximide-treated group, the transfected cells were harvested without further cycloheximide treatment. Each treatment was triplicated.

RNA isolation, reverse transcription–PCR (RT–PCR) and sequencing

Total RNA was prepared using a Purescript RNA Purification System (Gentra, Minneapolis, MN, USA). One microgram of RNA was used for reverse transcription using avian myeloblastosis virus reverse transcriptase and a human *SOD1*-specific primer (hSOD13′R: 5′-ctacagctagcaggataa cagatgag-3′). The synthesized first-strand cDNA fragments were PCR-amplified using two human *SOD1*-specific primers with an anchored *Eco*RI or *Xho*I restriction site, respectively (SOD1EcoRIf: 5′-cagtgaattcgaccagtgaaggtgtggg gaagc-3′, SOD1XhoIr: 5′-gatcctcgagccacctttgcccaagtcatctgc-3′). The RT–PCR product was agarose gel purified using QIAGEN Gel Extraction Kit (QIAGEN Science, MD, USA). An aliquot of the PCR product was directly sequenced using PCR primers. For subcloing, the rest of the PCR product was digested with *Eco*RI/*Xho*I and agarose-gel purified.

Subcloning and sequencing

The restriction enzyme-digested and purified *SOD1* cDNA fragments were subcloned into the *Eco*RI and *Xho*I sites of pBluescript plasmid vector. Bacterial clones with recombinant plasmid were randomly selected and cultured. Individual plasmid DNA was extracted and sequenced using a CEQ 8000 GeXP sequencer (Beckman Coulter Inc., Fullerton, CA, USA).

Dosage analysis

Plasmid DNA containing an *Eco*RI/*Xho*I cDNA fragment with a mutation (either E77X, K91X or T116X) was mixed with plasmid containing a wild-type *Eco*RI/*Xho*I cDNA fragment at 10 different ratios by amount, i.e. from 0.1 to 1.0 (mutant/wild-type). Mixed DNA samples were used as templates for PCR using the same protocol as that used in RT–PCR, and the PCR products were sequenced. The ratio of the peak height was established by measuring the individual peak height (T/G in 77X or T/A in 116X) at these 10 points with known plasmid DNA ratio (mutant/wild-type, 0.1–1.0). Triplicate experiments were performed and the mean ratios were taken to draw a standard curve and equation using Microsoft Excel. Similarly, the mean ratios (mutant/wild-type) of the peak height of the RT–PCR products were converted to percentage based on the standard curves and equations using wild-type SOD1 as 1 (100%).

Development of transgenic mice overexpressing mutant SOD1

The 11.6 kb *Eco*RI/*Bam*HI fragment containing the E77X or K91X mutation and the 10.5 kb *Eco*RI/*Bam*HI fragment containing the T116X mutation were released by *Eco*RI/*Bam*HI double digestion, agarose gel-purified and used for microinjection into fertilized eggs derived from a zygote of a C57BL/6 × SJL cross. Transgenic mice were initially identified by PCR by using human SOD1-specific primers at the 3′-UTR of the SOD1 gene (HSOD1-3′ forward, 5′-ccaataaa cattcccttggatg-3′; HSOD1-3′ reverse, 5′-caggatacatttctacagcta g-3′) and subsequently confirmed by southern blot. Potential homozygous mice were analyzed by southern blot. Onset of disease phenotype in mice is defined by showing more than one of the following signs: (i) fine tremor at one or more toes when suspended in the air; (ii) reduced spontaneous movement; (iii) failure to gain weight or loss of weight; (iv) poor grooming; (v) muscle weakness; and (vi) partial paralysis. End-stage of the disease is defined as when a mouse is paralyzed and cannot right by itself in 30 s after it is laid on one side. Animal-use protocols have been approved by the Institutional Animal Care and Use Committee of Northwestern University for this project.

Southern and northern blot analysis

For southern blot, five micrograms of mouse genomic DNA were digested with *Pst*I to completion, separated on a 0.8% agarose gel, and transferred to a nylon membrane. The membrane was dried for 2 h at 80°C. A genomic DNA fragment of 600 bp in size from intron 1 of human *SOD1* gene was used as a probe. This fragment was PCR-amplified using human SOD1-specific primers (hSOD1-spF: 5′-gttctaggtcatgattggg ctg-3′; hSOD1-spR: 5′-caccagttggtaacttcactaag-3′). The probe was labeled with dGTP-^{32}P by PCR. Hybridization was carried out using a hybridization solution (0.125 M Na2HPO3/0.25 M NaCl/7% SDS/1 mM EDTA/10% PEG) at 65°C for 18 h. The hybridized membrane was washed with 2X SSC/0.1% SDS for 30 min and 0.5X SSC/0.1% SDS for 30 min and then exposed to X-ray film. For northern blot, 15 micrograms of total RNA isolated from brain were separated on a 1% agarose gel containing formaldehyde, and transferred to a nylon membrane. The membrane was dried for 2 h at 80°C. For detection of human *SOD1* transgene expression, a human SOD1-specific probe was used. This probe, 78 bp in size from the 3′ untranslated region of human *SOD1*, was PCR amplified using two primers (hSOD1-3′F: 5′-ccaataaacattcccttggatgt-3′; hSOD1-3′R: 5′-caggatacatt tctacagctagc 3′). For the detection of mouse endogenous SOD1 expression, a mouse SOD1-specific probe was used. This probe, 94 bp in size from the 3′ untranslated region of mouse *SOD1*, was PCR amplified using two primers (mSOD1-3′F: 5′-gattgcgcagtaaacattccctgt-3′; mSOD1-3′R: 5′-cacagttacaactcttcagattac-3′).

Histopathological analysis

Mice deeply anesthetized with an intra-peritoneal injection of pentobarbarbital (0.15 mg/g) were sacrificed by total body perfusion with 60 ml of fresh saline followed by freshly prepared 4% paraformaldehyde in PBS. Brain and spinal cord were removed, postfixed in the same fixative, and embedded in paraffin. The sections were made at 6 μm for routine pathological examination and immunohistochemistry. For immunohistochemistry, the sections were deparaffinized and rehydrated

by passing the slides in serial solutions: three times for 10 min in xylene, three times for 5 min in 100% ethanol, three times for 3 min in 95% ethanol, once for 5 min each in 75% ethanol, 50% ethanol, deionized water and PBS, respectively. The antigens in the sections were retrieved using a decloaking chamber (Biocare Medical, Walnut Creek, CA, USA) with a retrieval solution (10 mM citrate acid, pH 6.0) for 20 min. The sections were cooled to room temperature for 30 min and rinsed with deionized water for 5 min. Possible intrinsic endogenous peroxidase activities were blocked with 2% hydrogen peroxide. Non-specific background was blocked with PBS/1% BSA for 20 min at room temperature. The specific primary antibody of interest (such as f-SOD1) was applied to the slides and incubated at room temperature for 1 h. After rinsing the slides, a biotinylated secondary antibody in PBS was applied, and the slides were incubated at room temperature for 30 min. After removing the excess secondary antibody, a peroxidase-conjugated streptavidin (BioGenex, San Ramon, CA, USA) was applied, and the slides were incubated for 30 min at room temperature. After rinsing, positive signals were developed by incubating the slides with 3-amino-9-ethylcarbazole chromogen. The slides were counterstained with appropriate counterstaining reagents and sealed with Aqua Poly/Mount (Polyscience, Warrington, PA, USA). The slides were examined and photographed under a light microscope.

Quantification of anterior horn motor neurons was performed on 9 μm transverse sections of lumbar spinal cord from L1 to L3, the lumbar enlargement in mice. In every third section, at least 20 sections total from each animal was immuno-stained with antibody against choline acetyltransferase (ChAT) (Chemicon International, Temecula, CA, USA). The areas of the anterior horn where motor neurons were counted included laminae VII, VIII and IX. Cells that met the following criteria in this area were counted as a motor neuron: (i) ChAT positive; (ii) cell body diameter over 15 μm; (iii) with a clearly defined cytoplasm containing nucleus and prominent nucleolus.

Confocal microscopy

Sections were prepared by using the same protocols as described in the *Histopathological Analysis*. After antigen retrieval, the sections were then blocked in a PBS solution containing 1% BSA for 1 h. Primary antibodies raised in different hosts (such as rabbit anti-SOD1, mouse anti-GFAP) were then applied with appropriate dilutions for 1 h followed by at least four 10 min wash steps before exposure to the secondary antibody solution (Pierce goat anti-mouse IgG conjugated with rhodamine and Chemicon goat anti-rabbit IgG conjugated with FITC at appropriate dilution). This was followed by four additional 10 min wash steps. The specimens were mounted in Antifade mounting media (Molecular Probes). Specimens were examined by using an LSM 510 META Laser Scanning Confocal Microscope with its multi-tracking setting. The same pinhole diameter was used to acquire each channel.

SUPPLEMENTARY MATERIAL

Supplementary Material is available at HMG Online.

ACKNOWLEDGEMENTS

We thank Janice Caliendo for proofreading this manuscript.

Conflict of Interest statement. None declared.

FUNDING

The authors acknowledge the support from the National Institutes of Health Grants NS40308 (H.-X.D.), NS050641 and NS046535 (T.S.); the Les Turner ALS Foundation, the National Organization for Rare Disorders, the Vena E. Schaff ALS Research Fund, a Harold Post Research Professorship, the Herbert and Florence C. Wenske Foundation, the Ralph and Marian Falk Medical Research Trust, an Abbott Labs Duane and Susan Burnham Professorship, and the David C. Asselin MD Memorial Fund (T.S.). Funding to pay the Open Access publication charges for this article was provided by the Les Turner ALS Foundation.

AUTHOR CONTRIBUTIONS

H.-X.D. and T.S. designed the research. H.-X.D., H.J., R.F., H.Z., Y.S. and M.H. developed the transgenic mice and performed genetic analysis; H.-X.D., H.Z., E.L., M.C.D.C. and T.S. did pathological analysis; H.-X.D. and T.S. analyzed data and wrote the paper.

REFERENCES

1. Rosen, D.R., Siddique, T., Patterson, D., Figlewicz, D.A., Sapp, P., Hentati, A., Donaldson, D., Goto, J., O'Regan, J.P., Deng, H.X. *et al.* (1993) Mutations in Cu/Zn superoxide dismutase gene are associated with familial amyotrophic lateral sclerosis. *Nature*, **362**, 59–62.
2. Deng, H.X., Hentati, A., Tainer, J.A., Iqbal, Z., Cayabyab, A., Hung, W.Y., Getzoff, E.D., Hu, P., Herzfeldt, B., Roos, R.P. *et al.* (1993) Amyotrophic lateral sclerosis and structural defects in Cu,Zn superoxide dismutase. *Science*, **261**, 1047–1051.
3. Gurney, M.E., Pu, H., Chiu, A.Y., Dal Canto, M.C., Polchow, C.Y., Alexander, D.D., Caliendo, J., Hentati, A., Kwon, Y.W., Deng, H.X. *et al.* (1994) Motor neuron degeneration in mice that express a human Cu,Zn superoxide dismutase mutation. *Science*, **264**, 1772–1775.
4. Reaume, A.G., Elliott, J.L., Hoffman, E.K., Kowall, N.W., Ferrante, R.J., Siwek, D.F., Wilcox, H.M., Flood, D.G., Beal, M.F., Brown, R.H., Jr *et al.* (1996) Motor neurons in Cu/Zn superoxide dismutase-deficient mice develop normally but exhibit enhanced cell death after axonal injury. *Nat. Genet.*, **13**, 43–47.
5. Deng, H.X., Shi, Y., Furukawa, Y., Zhai, H., Fu, R., Liu, E., Gorrie, G.H., Khan, M.S., Hung, W.Y., Bigio, E.H. *et al.* (2006) Conversion to the amyotrophic lateral sclerosis phenotype is associated with intermolecular linked insoluble aggregates of SOD1 in mitochondria. *Proc. Natl Acad. Sci. USA*, **103**, 7142–7147.
6. Furukawa, Y., Fu, R., Deng, H.X., Siddique, T. and O'Halloran, T.V. (2006) Disulfide cross-linked protein represents a significant fraction of ALS-associated Cu, Zn-superoxide dismutase aggregates in spinal cords of model mice. *Proc. Natl Acad. Sci. USA*, **103**, 7148–7153.
7. Kunst, C.B. (2004) Complex genetics of amyotrophic lateral sclerosis. *Am. J. Hum. Genet.*, **75**, 933–947.
8. Hardy, J. and Selkoe, D.J. (2002) The amyloid hypothesis of Alzheimer's disease: progress and problems on the road to therapeutics. *Science*, **297**, 353–356.
9. Supattapone, S., Bosque, P., Muramoto, T., Wille, H., Aagaard, C., Peretz, D., Nguyen, H.O., Heinrich, C., Torchia, M., Safar, J. *et al.* (1999) Prion protein of 106 residues creates an artifical transmission barrier for prion replication in transgenic mice. *Cell*, **96**, 869–878.

10. Frenkel, D., Balass, M. and Solomon, B. (1998) N-terminal EFRH sequence of Alzheimer's beta-amyloid peptide represents the epitope of its anti-aggregating antibodies. *J. Neuroimmunol.*, **88**, 85–90.
11. Bard, F., Cannon, C., Barbour, R., Burke, R.L., Games, D., Grajeda, H., Guido, T., Hu, K., Huang, J., Johnson-Wood, K. *et al.* (2000) Peripherally administered antibodies against amyloid beta-peptide enter the central nervous system and reduce pathology in a mouse model of Alzheimer disease. *Nat. Med.*, **6**, 916–919.
12. Taylor, J.P., Hardy, J. and Fischbeck, K.H. (2002) Toxic proteins in neurodegenerative disease. *Science*, **296**, 1991–1995.
13. Jonsson, P.A., Ernhill, K., Andersen, P.M., Bergemalm, D., Brannstrom, T., Gredal, O., Nilsson, P. and Marklund, S.L. (2004) Minute quantities of misfolded mutant superoxide dismutase-1 cause amyotrophic lateral sclerosis. *Brain*, **127**, 73–88.
14. Wang, J., Xu, G., Li, H., Gonzales, V., Fromholt, D., Karch, C., Copeland, N.G., Jenkins, N.A. and Borchelt, D.R. (2005) Somatodendritic accumulation of misfolded SOD1-L126Z in motor neurons mediates degeneration: alphaB-crystallin modulates aggregation. *Hum. Mol. Genet.*, **14**, 2335–2347.
15. Watanabe, Y., Yasui, K., Nakano, T., Doi, K., Fukada, Y., Kitayama, M., Ishimoto, M., Kurihara, S., Kawashima, M., Fukuda, H. *et al.* (2005) Mouse motor neuron disease caused by truncated SOD1 with or without C-terminal modification. *Brain Res. Mol. Brain Res.*, **135**, 12–20.
16. Maquat, L.E. (2004) Nonsense-mediated mRNA decay: splicing, translation and mRNP dynamics. *Nat. Rev. Mol. Cell Biol.*, **5**, 89–99.
17. Pereira, F.J., do Ceu Silva, M., Picanco, I., Seixas, M.T., Ferrao, A., Faustino, P. and Romao, L. (2006) Human alpha2-globin nonsense-mediated mRNA decay induced by a novel alpha-thalassaemia frameshift mutation at codon 22. *Br. J. Haematol.*, **133**, 98–102.
18. Wong, P.C., Pardo, C.A., Borchelt, D.R., Lee, M.K., Copeland, N.G., Jenkins, N.A., Sisodia, S.S., Cleveland, D.W. and Price, D.L. (1995) An adverse property of a familial ALS-linked SOD1 mutation causes motor neuron disease characterized by vacuolar degeneration of mitochondria. *Neuron*, **14**, 1105–1116.
19. Bruijn, L.I., Becher, M.W., Lee, M.K., Anderson, K.L., Jenkins, N.A., Copeland, N.G., Sisodia, S.S., Rothstein, J.D., Borchelt, D.R., Price, D.L. *et al.* (1997) ALS-linked SOD1 mutant G85R mediates damage to astrocytes and promotes rapidly progressive disease with SOD1-containing inclusions. *Neuron*, **18**, 327–338.
20. Beckman, J.S., Estevez, A.G., Crow, J.P. and Barbeito, L. (2001) Superoxide dismutase and the death of motoneurons in ALS. *Trends Neurosci.*, **24**, S15–S20.
21. Liochev, S.I. and Fridovich, I. (2003) Mutant Cu,Zn superoxide dismutases and familial amyotrophic lateral sclerosis: evaluation of oxidative hypotheses. *Free Radic. Biol. Med.*, **34**, 1383–1389.
22. Bruijn, L.I., Miller, T.M. and Cleveland, D.W. (2004) Unraveling the mechanisms involved in motor neuron degeneration in ALS. *Annu. Rev. Neurosci.*, **27**, 723–749.
23. Manfredi, G. and Xu, Z. (2005) Mitochondrial dysfunction and its role in motor neuron degeneration in ALS. *Mitochondrion*, **5**, 77–87.
24. Tiwari, A. and Hayward, L.J. (2005) Mutant SOD1 instability: implications for toxicity in amyotrophic lateral sclerosis. *Neurodegener. Dis.*, **2**, 115–127.
25. Rakhit, R. and Chakrabartty, A. (2006) Structure, folding, and misfolding of Cu,Zn superoxide dismutase in amyotrophic lateral sclerosis. *Biochim. Biophys. Acta*, **1762**, 1025–1037.
26. Culotta, V.C., Yang, M. and O'Halloran, T.V. (2006) Activation of superoxide dismutases: putting the metal to the pedal. *Biochim. Biophys. Acta*, **1763**, 747–758.
27. Kato, S., Hayashi, H., Nakashima, K., Nanba, E., Kato, M., Hirano, A., Nakano, I., Asayama, K. and Ohama, E. (1997) Pathological characterization of astrocytic hyaline inclusions in familial amyotrophic lateral sclerosis. *Am. J. Pathol.*, **151**, 611–620.
28. Yoshihara, T., Ishii, T., Iwata, M. and Nomoto, M. (1998) Ultrastructural and histochemical study of the motor end plates of the intrinsic laryngeal muscles in amyotrophic lateral sclerosis. *Ultrastruct. Pathol.*, **22**, 121–126.
29. Cha, C.I., Kim, J.M., Shin, D.H., Kim, Y.S., Kim, J., Gurney, M.E. and Lee, K.W. (1998) Reactive astrocytes express nitric oxide synthase in the spinal cord of transgenic mice expressing a human Cu/Zn SOD mutation. *Neuroreport*, **9**, 1503–1506.
30. Rafalowska, J. and Podlecka, A. (1998) Does the pathological factor in amyotrophic lateral sclerosis (ALS) damage also astrocytes? *Folia Neuropathol.*, **36**, 87–93.
31. Trotti, D., Rolfs, A., Danbolt, N.C., Brown, R.H., Jr and Hediger, M.A. (1999) SOD1 mutants linked to amyotrophic lateral sclerosis selectively inactivate a glial glutamate transporter. *Nat. Neurosci.*, **2**, 427–433.
32. Boillee, S., Yamanaka, K., Lobsiger, C.S., Copeland, N.G., Jenkins, N.A., Kassiotis, G., Kollias, G. and Cleveland, D.W. (2006) Onset and progression in inherited ALS determined by motor neurons and microglia. *Science*, **312**, 1389–1392.
33. Beers, D.R., Henkel, J.S., Xiao, Q., Zhao, W., Wang, J., Yen, A.A., Siklos, L., McKercher, S.R. and Appel, S.H. (2006) Wild-type microglia extend survival in PU.1 knockout mice with familial amyotrophic lateral sclerosis. *Proc. Natl Acad. Sci. USA*, **103**, 16021–16026.
34. Ghadge, G.D., Wang, L., Sharma, K., Monti, A.L., Bindokas, V., Stevens, F.J. and Roos, R.P. (2006) Truncated wild-type SOD1 and FALS-linked mutant SOD1 cause neural cell death in the chick embryo spinal cord. *Neurobiol. Dis.*, **21**, 194–205.
35. Fischer, L.R., Culver, D.G., Tennant, P., Davis, A.A., Wang, M., Castellano-Sanchez, A., Khan, J., Polak, M.A. and Glass, J.D. (2004) Amyotrophic lateral sclerosis is a distal axonopathy: evidence in mice and man. *Exp. Neurol.*, **185**, 232–240.
36. Gould, T.W., Buss, R.R., Vinsant, S., Prevette, D., Sun, W., Knudson, C.M., Milligan, C.E. and Oppenheim, R.W. (2006) Complete dissociation of motor neuron death from motor dysfunction by Bax deletion in a mouse model of ALS. *J. Neurosci.*, **26**, 8774–8786.
37. Wang, J., Xu, G., Slunt, H.H., Gonzales, V., Coonfield, M., Fromholt, D., Copeland, N.G., Jenkins, N.A. and Borchelt, D.R. (2005) Coincident thresholds of mutant protein for paralytic disease and protein aggregation caused by restrictively expressed superoxide dismutase cDNA. *Neurobiol. Dis.*, **20**, 943–952.